

LQG design scheme for multiple vibration controllers in a data center facility

Masayuki Kohiyama^{*1} and Minako Yoshida²

¹*Department of System Design Engineering, Keio University, Yokohama, Japan*

²*Formerly, Graduate School of Science and Technology, Keio University, Yokohama, Japan*

(Received October 26, 2013, Revised November 9, 2013, Accepted December 10, 2013)

Abstract. This study proposes a scheme to design control parameters for a data center facility with a vibration controller on its top floor and a secondary isolation device with its own vibration controller designed to protect vibration-sensitive computer equipment. The aim is to reduce the effects of acceleration and drift from an earthquake on computer servers placed on the isolation device that must operate during a seismic event. A linear elastic model is constructed and the evaluation function of the linear quadratic Gaussian (LQG) control is formulated. The relationship between the control parameters and the responses is examined, and based on the observations, a control parameter design scheme is constructed to reduce the responses of both the building and the computer server effectively.

Keywords: vibration control; isolation floor; computer center; function maintenance

1. Introduction

1.1 Background

Data center facilities are expected to operate uninterrupted even during a severe earthquake. Toward this end, servers are often set up on an isolation table or floor to dampen the vibration produced during an earthquake. Lambrou and Constantinou (1994) conducted experiments and simulations to show the significantly reduced response in a computer cabinet on an isolated floor. Alhan and Gavin (2005) conducted seismic risk analysis of a computer rack on an isolated floor in critical facilities both with and without a base isolation system and clarified that the isolation of vibration-sensitive equipment significantly increases reliability of the equipment. Liu and Warn (2012) investigated the seismic performance of floor isolation systems in steel plate shear wall structures.

However, if the drift experienced on the isolation device exceeds its allowable limit, the servers may fall or collide with other objects and suffer damage that would interrupt their functionality. Indeed, such damage has been observed during previous earthquakes such as the Great East Japan Earthquake (Japan Data Center Council 2013). To prevent this, a vibration control device can be used; Kasai *et al.* (2013) report the performance of seismic protection technologies during the

*Corresponding author, Associate Professor, E-mail: kohiyama@sd.keio.ac.jp

Great East Japan Earthquake.

With respect to isolation devices, Gavin and Zaicenco (2007) investigated the performance and reliability of semi-active equipment isolation and revealed that semi-active isolation systems can significantly reduce the peak response accelerations without substantially increasing the isolator displacements. A semi-active vibration control system can run with a smaller electric power supply than an active control system. Therefore, an uninterruptible power supply system can be used to ensure continuous operation. State-of-the-art reviews on semi-active systems have been reported by Spencer (1996), Symans and Constantinou (1999), and Datta (2003). Many practical examples of semi-active vibration control systems exist in Japan (Kurata *et al.* 1999, Yoshida 2001, Nagashima *et al.* 2011); furthermore, full-scale applications have been reviewed by Spencer and Nagarajaiah (2003). Studies are continuing to focus on this topic (Fukukita and Takahashi 2011, Lin *et al.* 2013, Mei *et al.* 2013).

Xu and Li (2006) proposed a passive hybrid platform, on which high-tech equipment is placed, to abate the acceleration response of equipment during an earthquake and serve as an actively controlled platform to reduce the velocity response of equipment under normal working conditions. An experimental study was also reported by Xu *et al.* (2008). Hamidi and El Naggari (2007) conducted numerical simulations to demonstrate the ability of a sliding concave foundation to reduce the acceleration response of equipment inside a building within an acceptable range of lateral displacement. Lu and Lin (2008) proposed a smart isolation system for protecting precision equipment that combines an isolation platform with a variable friction device, and they used numerical simulations to demonstrate that the system effectively reduces the equipment acceleration and prevents excessive isolator displacement in near-fault earthquakes. Fan *et al.* (2009) conducted shaking table tests of a steel frame with an equipment isolation system using a magneto-rheological damper and investigated effective control algorithms. Reggio and De Angelis (2013) investigated the optimal design and seismic effectiveness of an equipment isolation system with nonlinear hysteretic behavior. Shi *et al.* (2013) proposed semi-active control using linear quadratic regulator control with a frequency-dependent scheduled gain design for floor isolation systems to reduce the acceleration and displacement for both short- and long-period motions.

1.2 Aims and scope of study

The authors' research group previously studied a cooperative control system of a coupled system of a building and its equipment, both of which have a control device, and showed that this system can sufficiently reduce the response of a building–elevator rope system (Yoshida *et al.* 2012).

The present study focuses on a data center building that has two control devices for the building and a computer server. Specifically, this study focuses on a building that has a vibration controller on the top floor and a server on an isolation device with a semi-active oil damper working as a second vibration controller.

The study (1) investigates the performance improvement when communicating and sharing sensor-acquired response data between two control units, (2) investigates the relationship between the control parameters of linear quadratic Gaussian (LQG) controllers (Stengel 1994, Naidu 2003) and seismic responses, and (3) proposes a scheme to design parameters considering the maximum control force and this relationship.

2. Formulation of system equations

2.1 Model of target system

The building under investigation is a steel structure that has an active vibration control device (AVCD) installed on the top floor, such as an active mass damper, and a connecting control device inserted between building structures. In the building, a server computer is placed on an isolation device with a semi-active oil damper on a specific floor. Practically, vibration-sensitive equipment should not be placed near the top floor, which has a large response during an earthquake; a middle floor is selected in the present study. Fig. 1 illustrates the setup of these entities; the building structure is modeled by a mass–spring system with N_b degrees of freedom based on an empirical story-shear stiffness distribution, where N_b is the number of stories. The number of degrees of freedom of the coupled system of the building, isolation device, and server computer is $N = N_b + 2$.

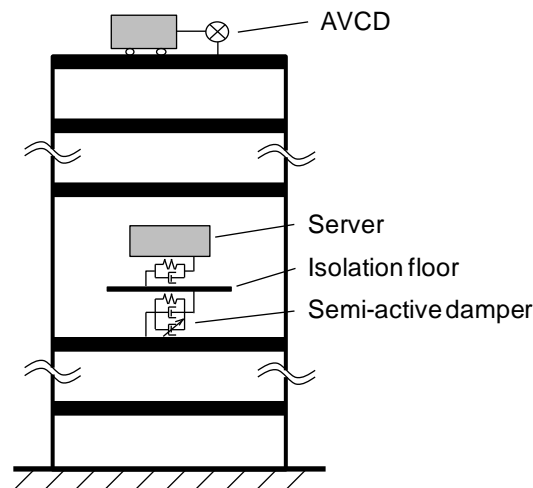


Fig. 1 Model of a building–server system

The system is assumed to show a linear elastic response. The equation of motion is given as follows:

$$\mathbf{M}\ddot{\mathbf{x}}_c(t) + \mathbf{C}\dot{\mathbf{x}}_c(t) + \mathbf{K}\mathbf{x}_c(t) = -\mathbf{M}\{1\}\ddot{z}(t) + \mathbf{f}\mathbf{u}(t) \tag{1}$$

where \mathbf{M} , \mathbf{C} , and \mathbf{K} are the mass, damping, and stiffness matrices of size $N \times N$, respectively. The vectors \mathbf{x}_c and \mathbf{u} denote the displacement of the system and control forces of the AVCD and semi-active oil damper, respectively, and the matrix \mathbf{f} represents location to apply the control forces. The sizes of \mathbf{x}_c , \mathbf{u} , and \mathbf{f} are $N \times 1$, $N_c \times 1$, and $N \times N_c$, respectively; in this study, the number of control forces N_c is 2 because the system has two vibration control devices. The variable z represents the ground displacement.

The equation of motion is converted into the following state-space representation:

$$\dot{\mathbf{x}}(t) = \mathbf{A}\mathbf{x}(t) + \mathbf{B}\mathbf{u}(t) + \mathbf{G}\ddot{z}(t) \tag{2}$$

where $\mathbf{x} = \{\mathbf{x}_c^T \quad \dot{\mathbf{x}}_c^T\}^T$ is the state vector and \mathbf{A} and \mathbf{B} are the system and input matrices, respectively. \mathbf{G} is a coefficient matrix for the ground acceleration. The sizes of \mathbf{A} , \mathbf{B} , and \mathbf{G} are $2N \times 2N$, $2N \times N_c$, and $2N \times 1$, respectively. In this study, the control force \mathbf{u} is calculated based on the LQG theory and the control scheme. With regard to the control scheme, Yoshida *et al.* (2012) classified control schemes for a building–equipment system (Fig. 2).

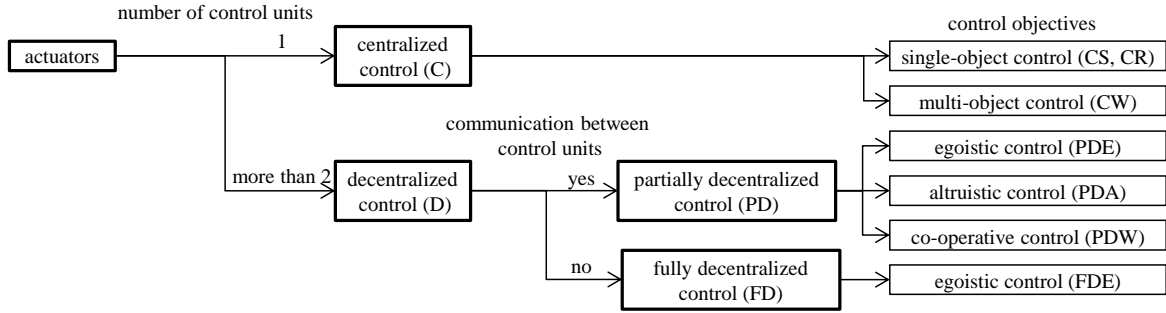


Fig. 2 Classification of control schemes for building–equipment system (Yoshida *et al.* 2012)

2.2 Centralized control

First, we explain the case of centralized control, where one control unit determines the control inputs of the AVCD and semi-active oil damper. The control force \mathbf{u} is calculated by the product of the control gain \mathbf{F}_{ctrl} and the estimated state vector $\hat{\mathbf{x}}(t)$ as follows:

$$\mathbf{u}(t) = -\mathbf{F}_{\text{ctrl}}\hat{\mathbf{x}}(t) \quad (3)$$

$$\dot{\hat{\mathbf{x}}}(t) = \mathbf{A}\hat{\mathbf{x}}(t) + \mathbf{B}\mathbf{u}(t) + \mathbf{F}_{\text{obs}}(\mathbf{y}_{\text{obs}}(t) - \hat{\mathbf{y}}_{\text{obs}}(t)) \quad (4)$$

$$\mathbf{y}_{\text{obs}}(t) = \mathbf{C}_{\text{obs}}\mathbf{x}(t) + \mathbf{D}_{\text{obs}}\mathbf{u}(t) + \mathbf{v}(t) \quad (5)$$

$$\hat{\mathbf{y}}_{\text{obs}}(t) = \mathbf{C}_{\text{obs}}\hat{\mathbf{x}}(t) + \mathbf{D}_{\text{obs}}\mathbf{u}(t) \quad (6)$$

where \mathbf{y}_{obs} and \mathbf{v} are the estimated sensor output and observation noise, respectively. The notation $(\hat{\cdot})$ represents a value estimated by an observer; in this study, a Kalman filter (Anderson and Moore 2005, Simon 2006) is employed as an observer. Eqs. (4) and (5) are the observer equation and sensor output equation, respectively. The coefficient matrix \mathbf{F}_{obs} is called the observer gain. The coefficient matrices \mathbf{C}_{obs} and \mathbf{D}_{obs} are given based on the allocation and type of sensors. The sizes of \mathbf{F}_{ctrl} , \mathbf{F}_{obs} , \mathbf{C}_{obs} , and \mathbf{D}_{obs} are $N_c \times 2N$, $2N \times N_s$, $N_s \times 2N$, and $N_s \times N_c$, respectively, in which N_s represents the number of sensors. We assume that the following physical quantities are acquired by sensors: isolation floor drift (isolation floor displacement relative to building floor on which it is placed), isolation floor acceleration relative to floor on which it is placed, server displacement relative to isolation floor on which it is placed, absolute velocity of building floors, and relative

acceleration of building floors to the ground. Note that the relative acceleration is determined by subtracting the ground acceleration from the absolute acceleration of a floor. We adopt the relative acceleration, rather than the absolute acceleration, to exclude a ground motion term from Eq. (4).

Because LQG controllers were adopted, the gains \mathbf{F}_{ctrl} and \mathbf{F}_{obs} are given as follows:

$$\mathbf{F}_{\text{ctrl}} = -\mathbf{R}^{-1}(\mathbf{S}^T + \mathbf{B}^T \mathbf{P}_{\text{ctrl}}) \quad (7)$$

$$\mathbf{F}_{\text{obs}} = \mathbf{P}_{\text{obs}} \mathbf{C}_{\text{obs}}^T \mathbf{V}^{-1} \quad (8)$$

where \mathbf{P}_{ctrl} and \mathbf{P}_{obs} are given by the solutions of the following Riccati equations, respectively.

$$\mathbf{P}_{\text{ctrl}} (\mathbf{A} - \mathbf{B} \mathbf{R}^{-1} \mathbf{S}^T) + (\mathbf{A} - \mathbf{B} \mathbf{R}^{-1} \mathbf{S}^T)^T \mathbf{P}_{\text{ctrl}} - \mathbf{P}_{\text{ctrl}} \mathbf{B} \mathbf{R}^{-1} \mathbf{B}^T \mathbf{P}_{\text{ctrl}} + \mathbf{Q} - \mathbf{S} \mathbf{R}^{-1} \mathbf{S}^T = \mathbf{O} \quad (9)$$

$$\mathbf{A} \mathbf{P}_{\text{obs}} + \mathbf{P}_{\text{obs}} \mathbf{A}^T - \mathbf{P}_{\text{obs}} \mathbf{C}_{\text{obs}}^T \mathbf{V}^{-1} \mathbf{C}_{\text{obs}} \mathbf{P}_{\text{obs}} + \mathbf{G} \mathbf{W} \mathbf{G}^T = \mathbf{O} \quad (10)$$

In Eq. (10), the matrices \mathbf{V} and \mathbf{W} are the power spectrum density of the observation noise and ground motion, respectively. The size of \mathbf{P}_{ctrl} and \mathbf{P}_{obs} is $2N \times 2N$ and the size of \mathbf{V} is $N_s \times N_s$. We assume the observation noise and ground motion as white noise processes. In Eqs. (7) and (9), the matrices \mathbf{Q} , \mathbf{S} , and \mathbf{R} are those in the following cost function (J), which is minimized by the LQG controller:

$$J = E[\mathbf{y}_{\text{ctrl}}^T(t) \mathbf{y}_{\text{ctrl}}(t) + \mathbf{u}^T(t) \mathbf{R} \mathbf{u}(t)] = E[\mathbf{x}^T(t) \mathbf{Q} \mathbf{x}(t) + 2\mathbf{x}^T(t) \mathbf{S} \mathbf{u}(t) + \mathbf{u}^T(t) \mathbf{R} \mathbf{u}(t)] \quad (11)$$

where the control output \mathbf{y}_{ctrl} is given by the control objective equation:

$$\mathbf{y}_{\text{ctrl}}(t) = \mathbf{C}_{\text{ctrl}} \mathbf{x}(t) + \mathbf{D}_{\text{ctrl}} \mathbf{u}(t) \quad (12)$$

and the matrices \mathbf{C}_{ctrl} and \mathbf{D}_{ctrl} are selectively given based on control objectives, i.e., objective responses to be suppressed by the controllers. The sizes of \mathbf{Q} , \mathbf{S} , \mathbf{R} , \mathbf{y}_{ctrl} , \mathbf{C}_{ctrl} , and \mathbf{D}_{ctrl} are $2N \times 2N$, $2N \times N_c$, $N_c \times N_c$, $N_o \times 1$, $N_o \times 2N$, and $N_o \times N_c$, respectively, in which N_o represents the number of control objectives.

In this study, the absolute acceleration of building floors, $\mathbf{y}_{\text{bldctrl}}$, is chosen for suppression of the building response and the drift of the isolation device, $\mathbf{y}_{\text{srvctrl}}$, is chosen for suppression of the server response.

$$\mathbf{y}_{\text{bldctrl}}(t) = \mathbf{C}_{\text{bldctrl}} \mathbf{x}(t) + \mathbf{D}_{\text{bldctrl}} \mathbf{u}(t) \quad (13)$$

$$\mathbf{y}_{\text{srvctrl}}(t) = \mathbf{C}_{\text{srvctrl}} \mathbf{x}(t) + \mathbf{D}_{\text{srvctrl}} \mathbf{u}(t) \quad (14)$$

Using two control outputs for the building and computer server responses, the cost function is formulated as follows:

$$J = E[\alpha \frac{\mathbf{y}_{\text{bldctrl}}^T(t) \mathbf{y}_{\text{bldctrl}}(t)}{N_b \bar{y}_{\text{bld}}^2} + (1 - \alpha) \frac{\mathbf{y}_{\text{srvctrl}}^T(t) \mathbf{y}_{\text{srvctrl}}(t)}{\bar{y}_{\text{srv}}^2} + \mathbf{u}^T(t) \mathbf{R} \mathbf{u}(t)] \quad (15)$$

where α is a weighting factor; when $\alpha = 1$, the cost function contains only the building response term and the controller primarily aims to suppress the building response, and when $\alpha = 0$, the computer server is the primary response. The constants, N_b , \bar{y}_{bld} , and \bar{y}_{srv} respectively denote the number of building floors and standard responses of a building and a server, and they are derived from a response analysis result with no control condition under a design input ground motion. In Eq. (15), the diagonal matrix \mathbf{R} consists of weighting parameters R_b for the building AVCD and R_s for the semi-active damper for the server. Thus, three weighting parameters have to be determined: α , R_b , and R_s .

2.3 Partially decentralized control

Next, we explain the case of partially decentralized control in which two control units determine the control inputs of the AVCD and semi-active oil damper, respectively. The two control units communicate and share parts of the sensor's output data. The control force \mathbf{u} has components u_p and u_s , which represent the control forces of the AVCD and semi-active oil damper, and they are calculated by the two control units as follows:

$$u_p(t) = -\mathbf{F}_{\text{pctrl}} \hat{\mathbf{x}}_p(t) \quad (16)$$

$$u_s(t) = -\mathbf{F}_{\text{sctrl}} \hat{\mathbf{x}}_s(t) \quad (17)$$

$$\dot{\hat{\mathbf{x}}}_p(t) = \mathbf{A} \hat{\mathbf{x}}_p(t) + \mathbf{B}_p u_p(t) + \mathbf{F}_{\text{pobs}} (\mathbf{y}_{\text{pobs}}(t) - \hat{\mathbf{y}}_{\text{pobs}}(t)) \quad (18)$$

$$\dot{\hat{\mathbf{x}}}_s(t) = \mathbf{A} \hat{\mathbf{x}}_s(t) + \mathbf{B}_s u_s(t) + \mathbf{F}_{\text{sobs}} (\mathbf{y}_{\text{sobs}}(t) - \hat{\mathbf{y}}_{\text{sobs}}(t)) \quad (19)$$

$$\mathbf{y}_{\text{pobs}}(t) = \mathbf{C}_{\text{pobs}} \mathbf{x}(t) + \mathbf{D}_{\text{pobs}} \mathbf{u}(t) + \mathbf{v}_p(t) \quad (20)$$

$$\mathbf{y}_{\text{sobs}}(t) = \mathbf{C}_{\text{sobs}} \mathbf{x}(t) + \mathbf{D}_{\text{sobs}} \mathbf{u}(t) + \mathbf{v}_s(t) \quad (21)$$

$$\hat{\mathbf{y}}_{\text{pobs}}(t) = \mathbf{C}_{\text{pobs}} \hat{\mathbf{x}}_p(t) + \mathbf{D}_{\text{pobs}} u_p(t) \quad (22)$$

$$\hat{\mathbf{y}}_{\text{sobs}}(t) = \mathbf{C}_{\text{sobs}} \hat{\mathbf{x}}_s(t) + \mathbf{D}_{\text{sobs}} u_s(t) \quad (23)$$

where the subscripts p and s represent values related to control units for the control of a building (primary system) and an isolation floor (secondary system). We assume, through the communication of sensor-acquired data between two control units, that the primary system control unit can use the isolation floor drift and relative acceleration, server relative displacement and acceleration, absolute velocity of building floors, and relative acceleration of building floors to the ground and that the secondary system control unit can use the isolation floor drift and relative acceleration, server relative displacement and acceleration, and absolute velocity and relative acceleration of the server-accommodating floor and the upper and lower floors of the server-accommodating floor.

The gains $\mathbf{F}_{\text{pctrl}}$, $\mathbf{F}_{\text{sctrl}}$, \mathbf{F}_{pobs} , and \mathbf{F}_{sobs} are respectively given as follows:

$$\mathbf{F}_{p\text{ctrl}} = -\mathbf{R}_p^{-1}(\mathbf{S}_p^T + \mathbf{B}^T \mathbf{P}_{p\text{ctrl}}) \quad (24)$$

$$\mathbf{F}_{s\text{ctrl}} = -\mathbf{R}_s^{-1}(\mathbf{S}_s^T + \mathbf{B}^T \mathbf{P}_{s\text{ctrl}}) \quad (25)$$

$$\mathbf{F}_{p\text{obs}} = \mathbf{P}_{p\text{obs}} \mathbf{C}_{p\text{obs}}^T \mathbf{V}_p^{-1} \quad (26)$$

$$\mathbf{F}_{s\text{obs}} = \mathbf{P}_{s\text{obs}} \mathbf{C}_{s\text{obs}}^T \mathbf{V}_s^{-1} \quad (27)$$

where $\mathbf{P}_{p\text{ctrl}}$, $\mathbf{P}_{s\text{ctrl}}$, $\mathbf{P}_{p\text{obs}}$, and $\mathbf{P}_{s\text{obs}}$ are given by the solutions of the Riccati equations in a manner similar to that in Eqs. (9) and (10). Here, the two cost functions are defined and used for the primary and secondary control units.

With respect to the control design parameters, three weighting parameters α , R_b , and R_s are defined in the same manner as in centralized control adopting the same control outputs.

2.4 Fully decentralized control

Finally, in fully decentralized control, two control units independently determine the control inputs of the AVCD and semi-active oil damper, and these units do not communicate or share the sensor's output data. We assume that the primary system control unit can use the absolute velocity and relative acceleration of building floors, and aims to suppress the building response only. With respect to the secondary system control unit, we assume that it can use the isolation floor drift and relative acceleration, server relative displacement and acceleration, and absolute velocity and relative acceleration of the server-accommodating floor, and aims to suppress the drift of the isolation device only.

Because the primary system control unit cannot obtain the isolation table state and the secondary system control unit cannot obtain the building floor response other than the server-accommodating floor, the control outputs of the primary and secondary system control units are defined independently. Consequently, two weighting parameters R_b and R_s remain as control design parameters. In fully decentralized control, the secondary system is assumed to simply receive an input from the primary system, such as a ground motion, and it is designed in the same manner as a conventional base-isolated building with a semi-active oil damper. This design approach is primitive and may appear so in practice. However, compared with centralized control, better control performance cannot be expected because the interaction between the primary and the secondary systems is neglected. The response of the secondary system depends on the dynamic characteristics of the primary structure (Villaverde 1997).

3. Case study

3.1 Model parameters

The target system is a 15-story data center that houses a server, with an isolation device placed on the 9th floor. Table 1 lists the model parameters of the target system. The semi-active oil damper for a server can change its damping coefficient from 30 to 300 Ns/m. For the calculation

of damping force, the ideal damping coefficient ($c_{s \text{ ideal}}$) is first determined by an ideal control force $u_{s \text{ ideal}}$, which is given by Eq. (3), using the following equation:

$$c_{s \text{ ideal}} = -\frac{u_{s \text{ ideal}}}{v_s} \quad (28)$$

where v_s is the relative velocity at an isolation device. When $c_{s \text{ ideal}}$ is outside the range of the semi-active oil damper (30–300 Ns/m), the actual damping coefficient is set to the limit value (30 or 300 Ns/m) that is nearer to $c_{s \text{ ideal}}$. Because the damping coefficient cannot be negative, the minimum damping coefficient is determined when the signs of the control force and the relative velocity at an isolation device are the same. When the absolute value of the control force exceeds the release load, the actual damping coefficient is set to be the minimum damping coefficient.

Table 1 Model parameters

Component	Parameter	Value
Building	Number of stories	15
	Mass of each layer	1×10^6 kg
	Story height	5 m
	Fundamental period	2 s
	Damping factor of 1st mode	0.02
AVCD for building	Installed location	15th layer mass (top)
	Maximum force	300 kN
Server computer	Placed location	8th layer mass (9th floor)
	Mass	400 kg
	Natural period	0.3 s
	Damping factor	0.01
Isolation device	Mass	50 kg
	Natural period	3.5 s
	Damping factor	0.50
Semi-active oil damper for isolation device	Minimum damping coefficient	30 Ns/m
	Maximum damping coefficient	300 Ns/m
	Release load	400 N
	Maximum force	500 N

3.2 Analysis result

To investigate the relation between the weighting parameters and the system responses, a time-history analysis was carried out. The following four input ground motions, scaled to have peak velocities of 0.25 m/s, were input into the model: three records of El Centro 1940 NS, Taft 1952 EW, Hachinohe 1968 NS, and one simulated ground motion based on the “Level-1” design

response spectrum prescribed by Notification No. 1461 of the Ministry of Construction, May 31, 2000, in Japan. Table 2 lists the maximum responses when the system have no control device.

Table 2 Maximum responses when the system does not have control devices

Response	Input ground motion			
	El Centro 1940 NS	Taft 1952 EW	Hachinohe 1968 NS	Simulated ground motion
Building acceleration [m/s ²]	4.729	5.070	3.503	1.397
Story drift angle of building [rad]	0.004619	0.004394	0.004126	0.001604
Server acceleration [m/s ²]	1.296	0.9632	1.429	0.4315
Drift of isolation device [m]	0.2044	0.1298	0.2388	0.08376

Figs. 3, 4, and 5 show the distribution of the maximum responses under the input ground motion of the scaled El Centro record using a centralized control with $\alpha = 0.5$, partially decentralized control with $\alpha = 0.5$, and fully decentralized control, respectively. The horizontal axes are the logarithm of the weighting parameter for the control force of the building (R_b) and the vertical axes are the logarithm of the server response (R_s). The white areas represent regions where either of the two control forces exceeded their maximum force limit, i.e., where saturation of the control force occurred.

It was observed that the building responses decreased more when a larger control force was applied, unless the control force was not saturated. However, the server acceleration response increased when a larger control force was applied. This tendency was observed under any input ground motion, control scheme, or control objective. Thus, the R_s value should be selected considering this trade-off relationship.

In Figs. 3, 4, and 5 (c), the drift of the isolation device decreased more when a larger AVCD control force was applied under all control schemes. This means that the AVCD control force effectively reduced the drift of the isolation device as well as the building response because the cost function in Eq. (15) includes both response terms when $\alpha = 0.5$. In the case of fully decentralized control, the cost function of AVCD does not include the term of the drift of the isolation device, and thus, the decrease in the gradient of the response in the horizontal direction is rather gentle; this is because the decrease in the drift results from the subsidiary effect of the reduced building response.

Figs. 6, 7 and 8 show the distribution of the maximum responses under all four input ground motions using a centralized control with $\alpha = 0, 0.5, \text{ and } 1$, respectively. In these figures, the white areas represent regions where saturation of the control force occurs under any of the four input ground motions.

A comparison of Figs. 6 and 7 shows that although the distributions are different, the minimum drifts of the isolation device are almost identical (0.17 m). On the other hand, Fig. 8 shows a larger drift of the isolation device (~ 0.21 m), and R_s does not influence the response. This is because the cost function of control J , Eq. (15), does not include the term of the drift of the isolation device

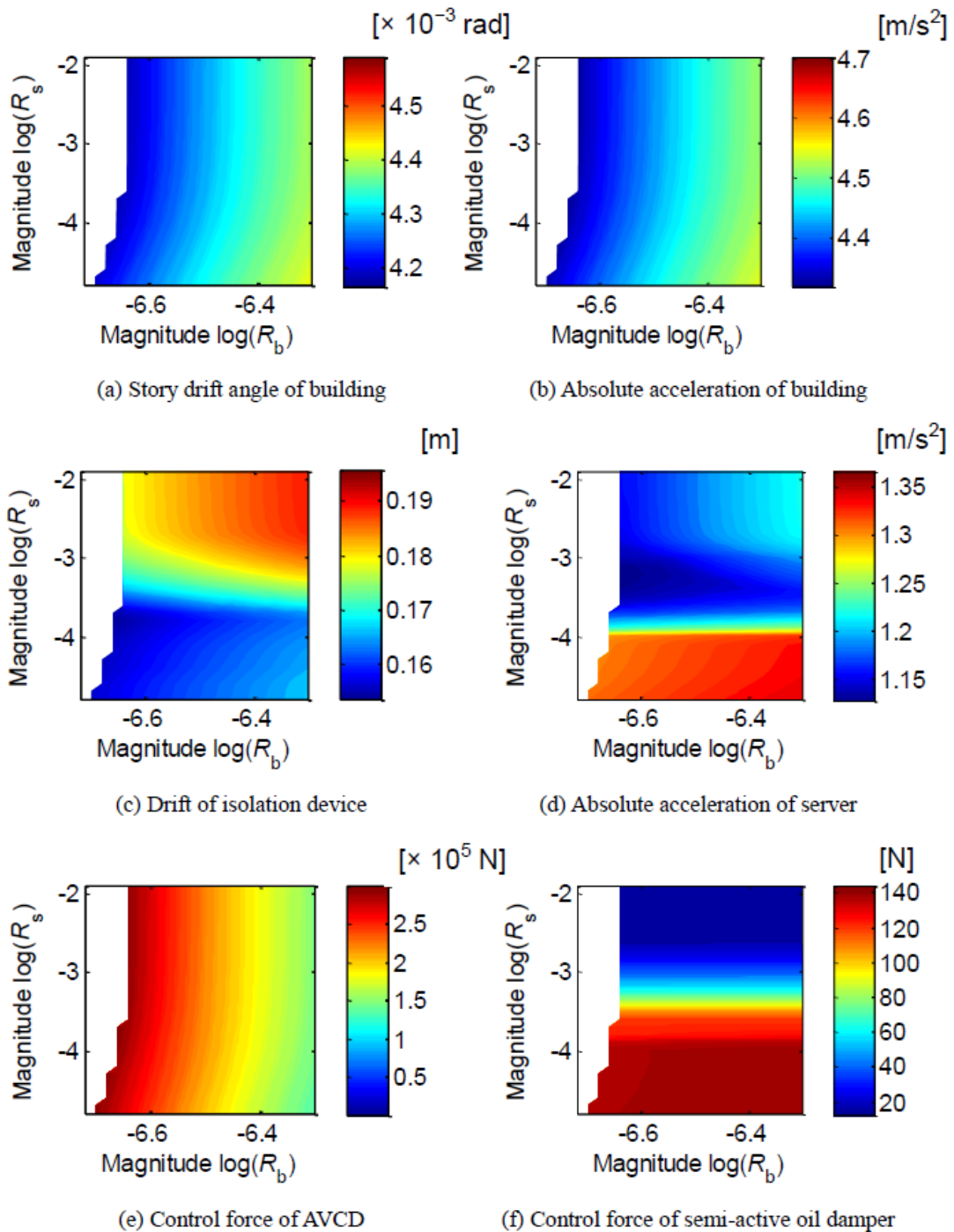


Fig. 3 Distribution of maximum response (input ground motion: El Centro, control scheme: centralized control, and $\alpha = 0.5$)

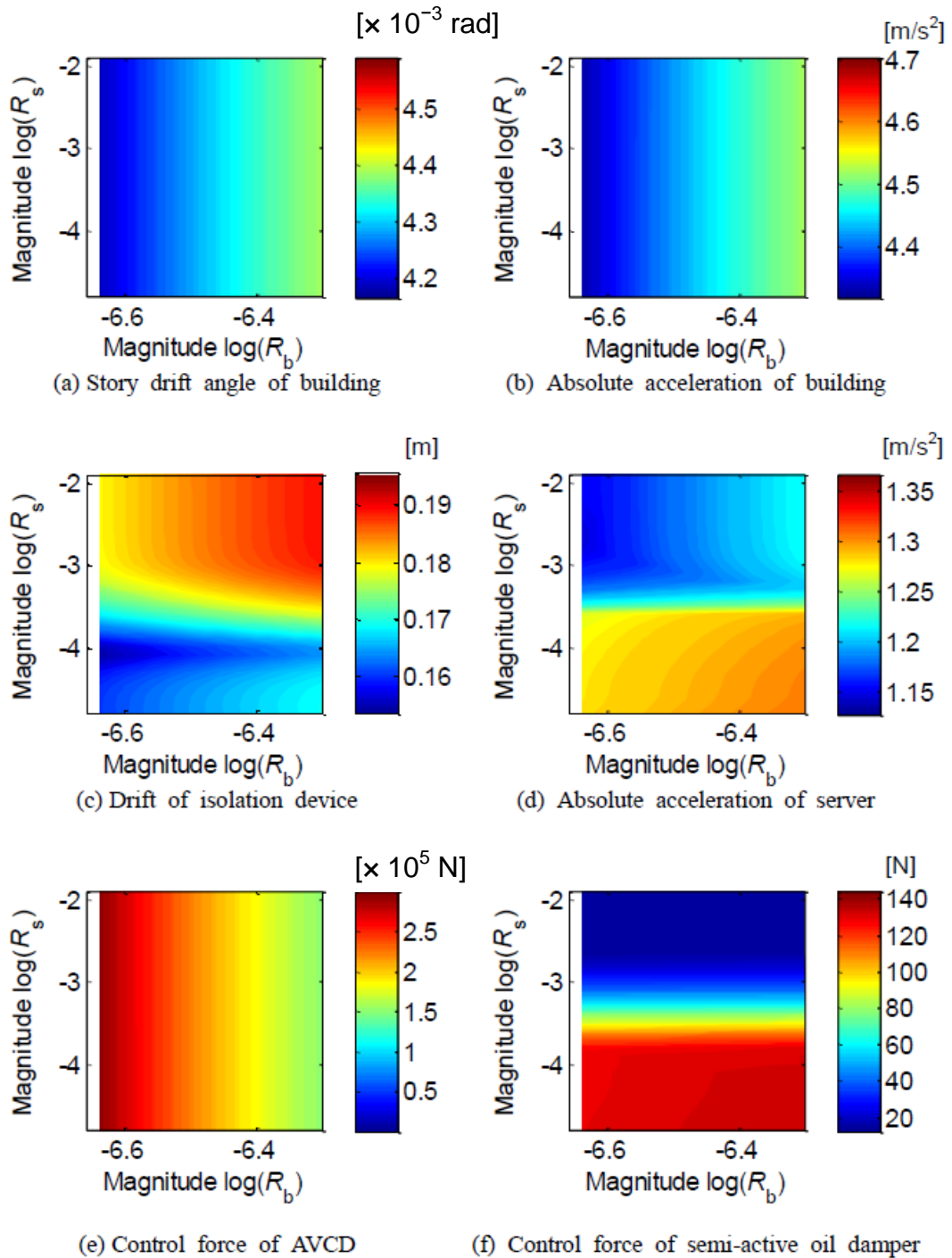


Fig. 4 Distribution of maximum response (input ground motion: El Centro, control scheme: partially decentralized control, and $\alpha = 0.5$)

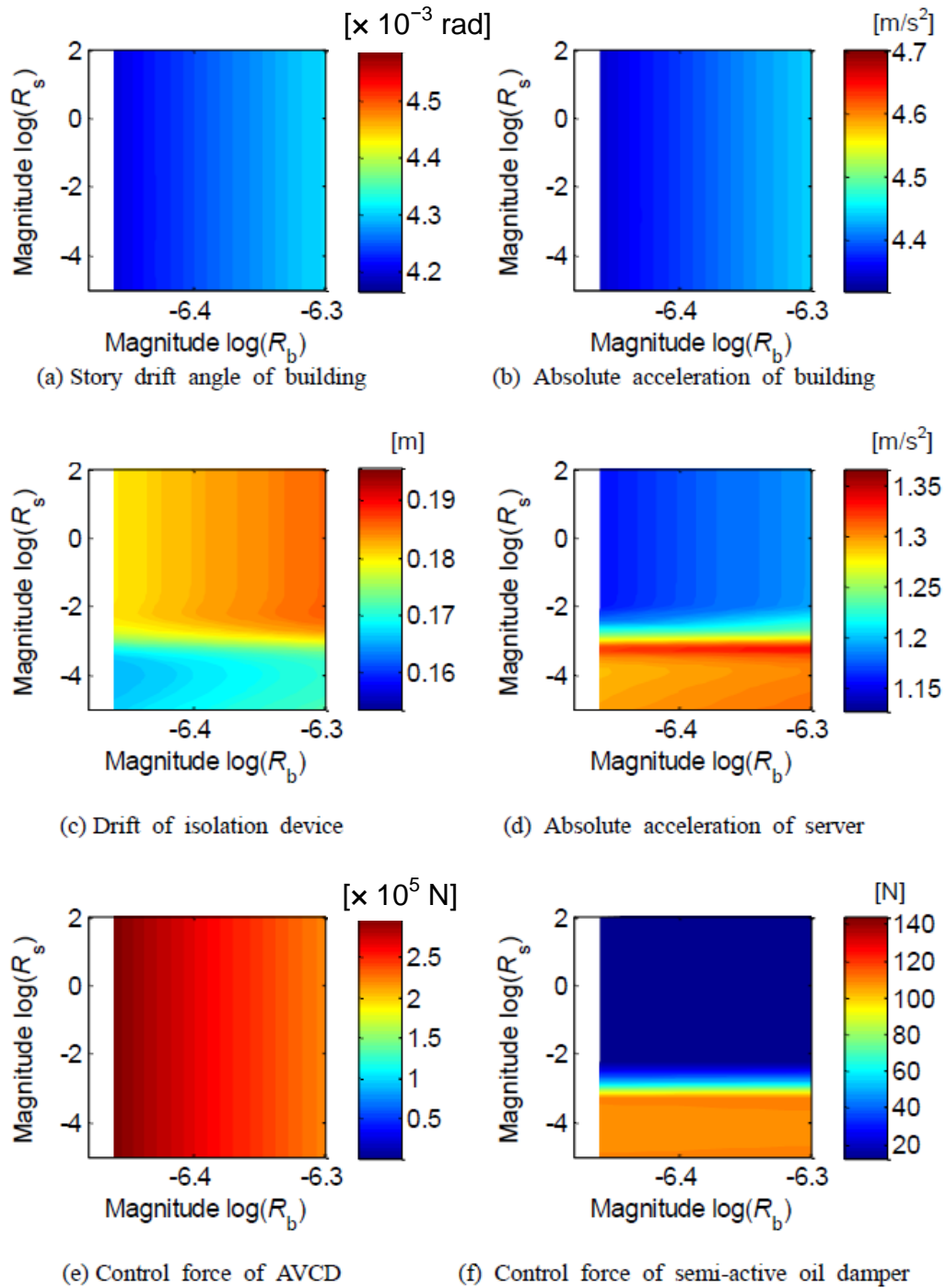


Fig. 5 Distribution of maximum response (input ground motion: El Centro, control scheme: fully decentralized control)

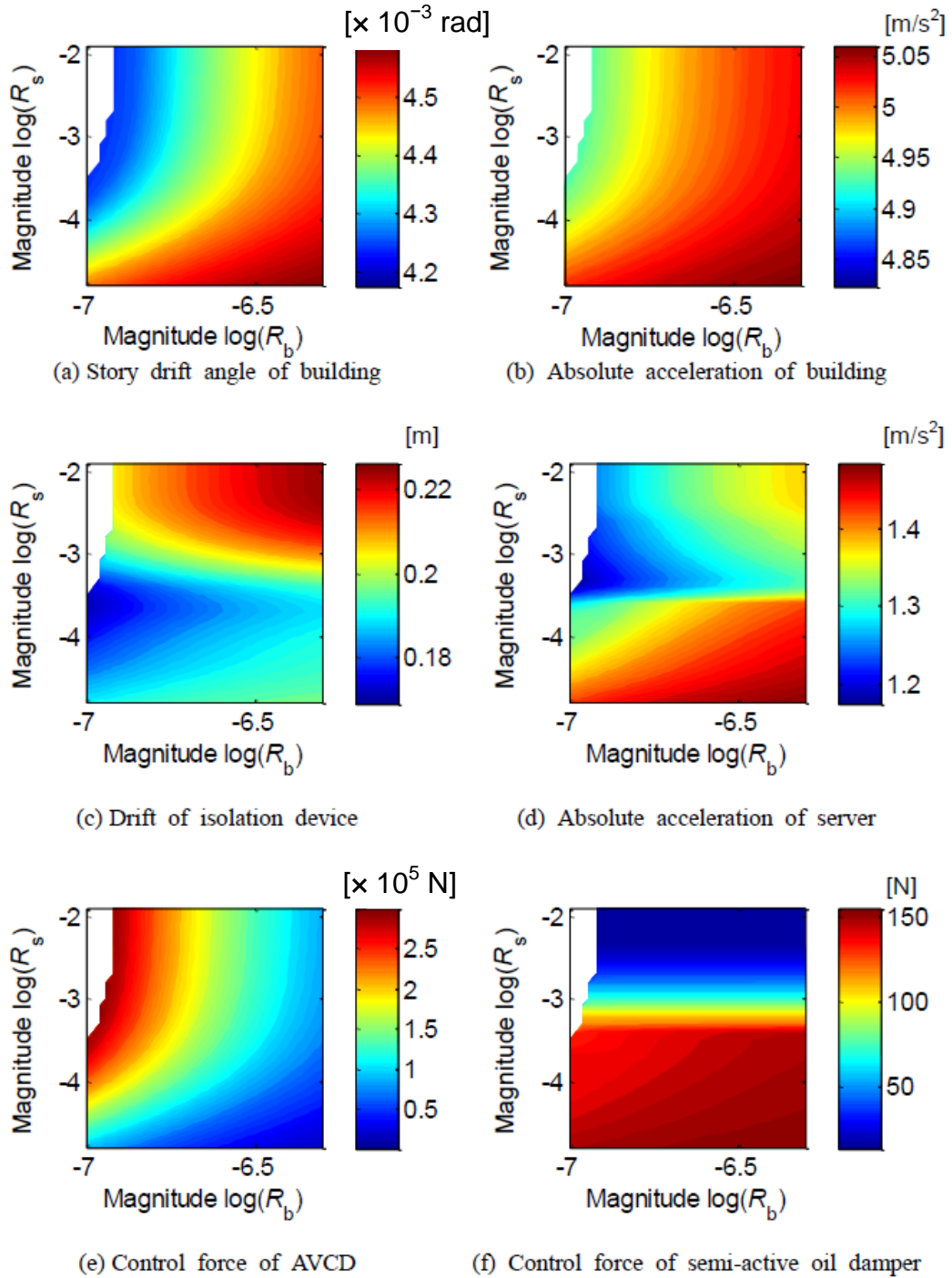


Fig. 6 Distribution of maximum response (input ground motion: all waves, control scheme: centralized control, and $\alpha = 0$)

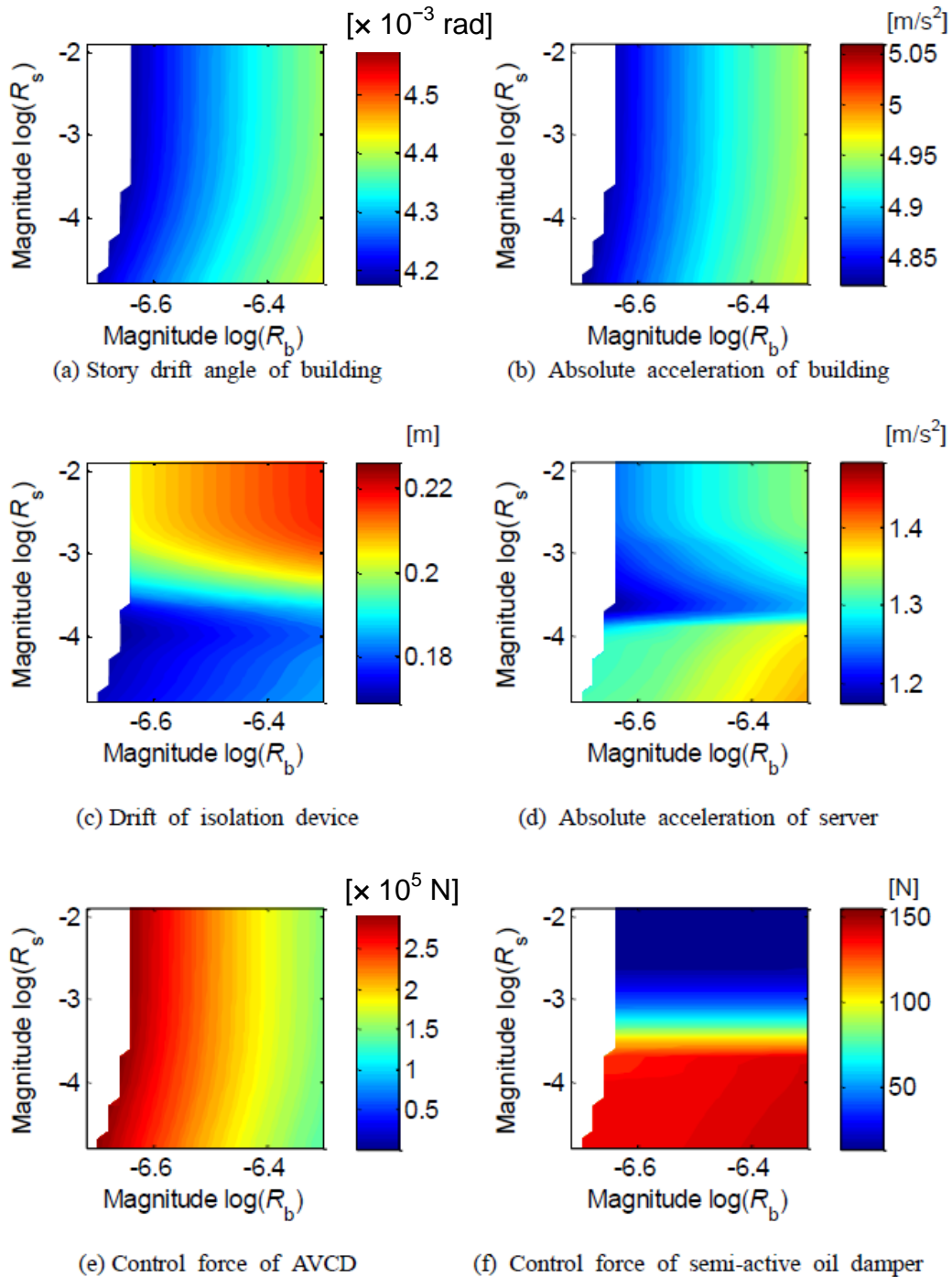


Fig. 7 Distribution of maximum response (input ground motion: all waves, control scheme: centralized control, and $\alpha = 0.5$)

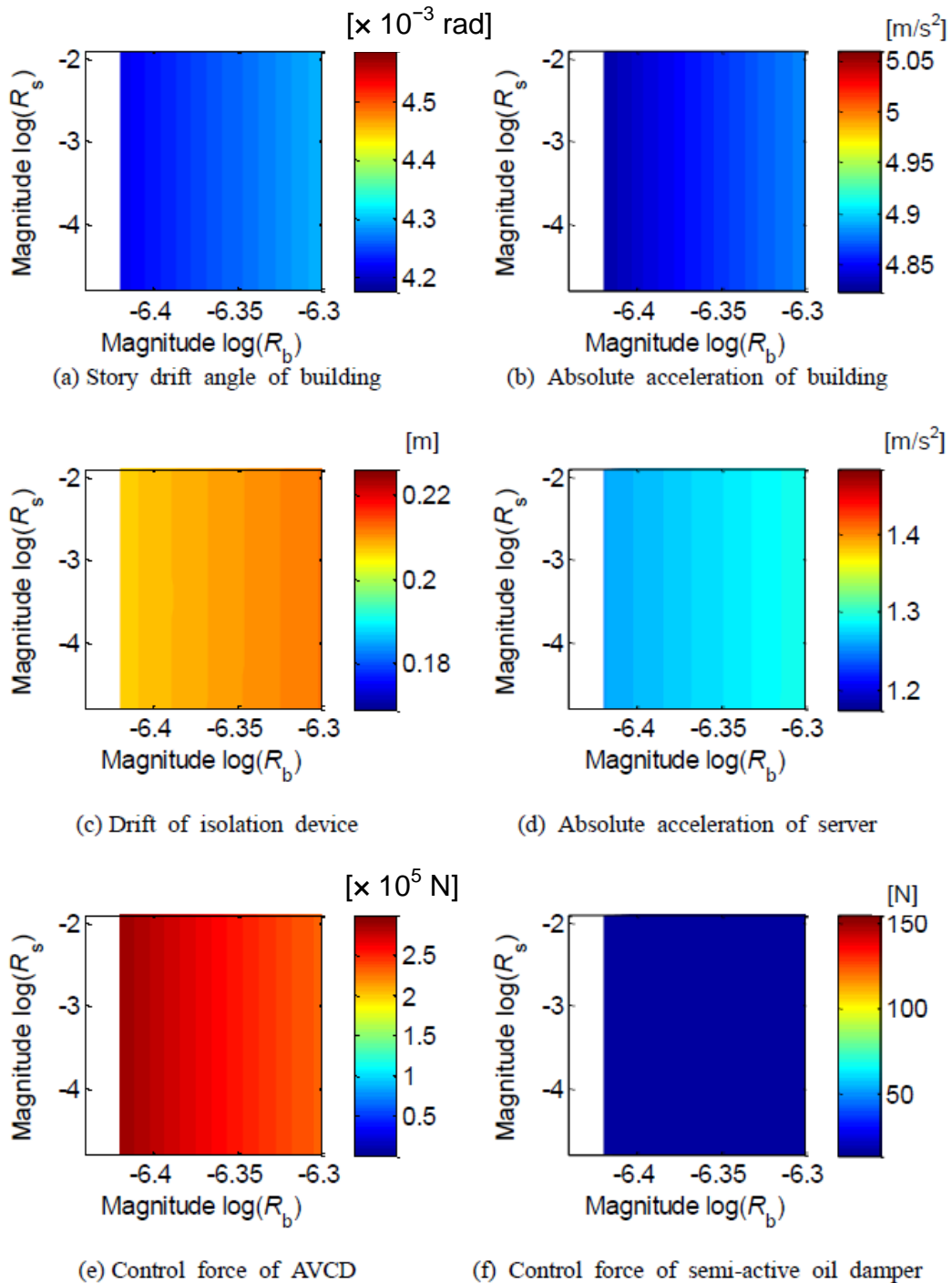


Fig. 8 Distribution of maximum response (input ground motion: all waves, control scheme: centralized control, and $\alpha = 1$)

when $\alpha = 1$. Hence, the inclusion of the term of the drift of the isolation device effectively reduces this response.

If the criteria of the server responses are set up as the maximum drift of the isolation device being less than 0.2 m and the maximum acceleration of the server being less than 2 m/s^2 , we can focus on the drift of the isolation device because the server acceleration is satisfied in all the cases. Fig. 9 shows a plot of the normalized response–weighting factor relation when the drift of the isolation device is minimum, in which the maximum responses under four input ground motions are normalized by the following threshold values: 3 m/s^2 for building acceleration, 0.005 rad for story drift, 2 m/s^2 for server acceleration, 0.2 m for drift of the isolation device, 300 kN for control force of AVCD, and 500 N for control force of semi-active oil damper. With regard to the control scheme, solid and dotted lines indicate centralized control and partially decentralized control, respectively, and asterisks indicate fully decentralized control. It is observed that centralized control with $\alpha < 1$ can best suppress the drift of the isolation device, and partially decentralized

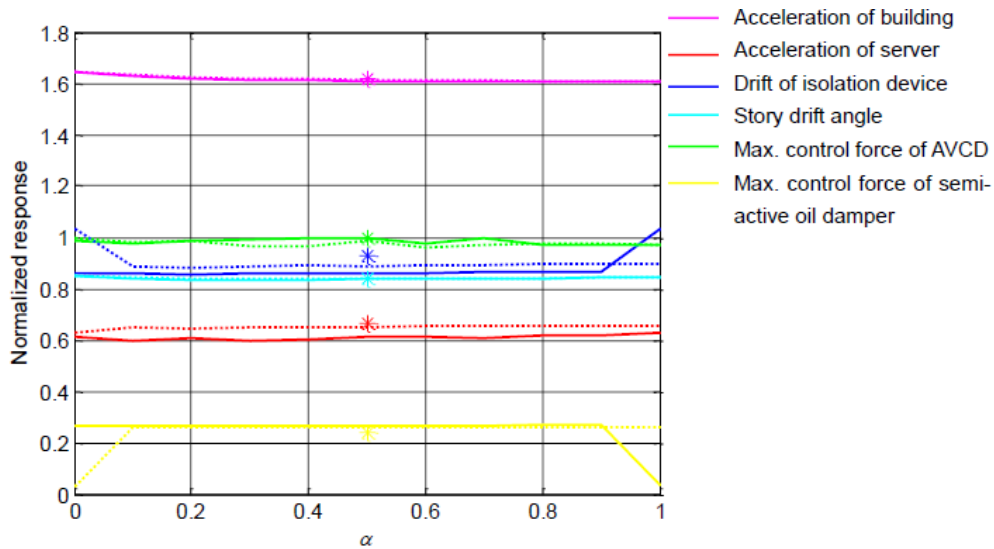


Fig. 9 Normalized response–weighting factor relation (solid line: centralized control, dotted line: partially decentralized control, and asterisk: fully decentralized control)

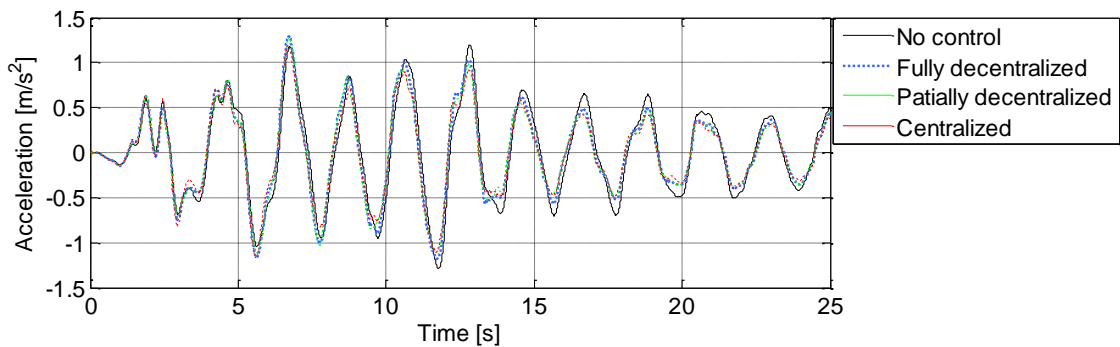


Fig. 10 Time-history of absolute acceleration of server (input ground motion: El Centro and $\alpha = 0.5$)

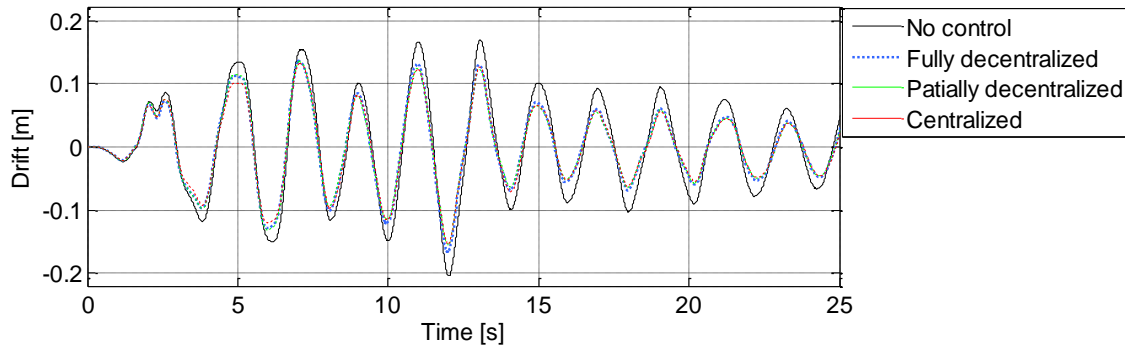


Fig. 11 Time-history of drift of isolation device (input ground motion: El Centro and $\alpha = 0.5$)

control with $\alpha > 0$ shows comparative performance. The normalized response of the drift of the isolation device is almost one under fully decentralized control, and we can conclude that building response information is useful for control to suppress the drift of the isolation device.

With regard to centralized control, the α value difference is not sensitive to reduce the drift when $\alpha < 1$. This is because a combination of R_b and R_s can substitute the weighting parameter α . Although the first term of the building response in Eq. (15) includes a quadratic term of control force, which is derived from Eq. (13), this term value is adjusted by the values of R_b and R_s . Consequently, we can give any value except one for α in the control parameter design.

Figs. 10 and 11 show a comparison of the response time-histories of the absolute acceleration of the server and the drift of the isolation device under the scaled El Centro wave with $\alpha = 0.5$, respectively. Except for several acceleration peaks in the initial phase up to $t = 6.7$ s, the responses are successfully suppressed by the controls, especially by centralized control. Note that an LQG assumes a stationary response in the derivation of the control gain, and it aims to minimize a quadratic cost function rather than the maximum response; thus, good performance is observed in the phase when the amplitude of the input ground motion is continuously large. When the maximum responses occur at around $t = 12$ s, the centralized and partially decentralized controls reduce the response well, and they show superior performance compared to decentralized control. A similar tendency was observed in the cases of other input ground motions. These results suggest that the response reduction performance can be improved by communicating and sharing sensor-acquired response data between two control units.

4. Design scheme of control parameters

Based on the observations in the previous section, a scheme for the control parameters design shown in Fig. 12 is proposed. First, an arbitrary α value is selected, e.g., $\alpha = 0.5$, so that the cost function of control includes both building and server response terms in Eq. (15). Then, the R_b value is determined, which does not cause saturation of the control force, because the acceleration response of a building, the primary system, can be effectively reduced, which consequently reduces the response of a server, the secondary system. Finally, the R_s value is selected considering the trade-off relation between the drift of the isolation device and the server acceleration.

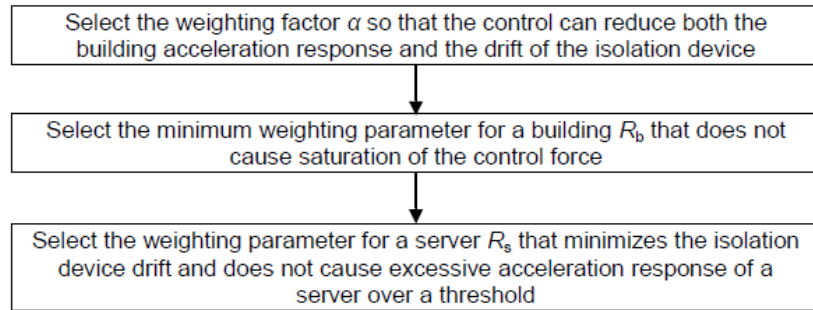


Fig. 12 Flowchart to design control parameters

5. Conclusions

This study proposed a design scheme of control parameters for a data center facility housing a building–equipment system with multiple control devices, namely, an active vibration control device on the top floor of the building and an isolation floor and a semi-active oil damper for a server computer. A linear elastic model of a coupled system including the building and server was constructed, and the evaluation function of LQG control was formulated for centralized control, partially decentralized control, and fully decentralized control. Using four input ground motions, dynamic analysis was carried out for possible combinations of the control parameter values, and the relationship between control parameters and responses was investigated.

It was revealed that large control force of an active vibration control device for a building could suppress both the story drift and the floor acceleration of the building; however, the server acceleration response increased when a larger control force was applied with a semi-active oil damper. Hence, it is important to consider the trade-off relation between the drift of the isolation device for a server and the server acceleration response. Based on the observations of the relation between control parameters and responses, a scheme to design control parameters is proposed to effectively suppress the objective responses considering the capacity of control devices and efficiency of the control forces.

Among the three control schemes—centralized control, partially decentralized control, and fully decentralized control—centralized control could best suppress the drift of the isolation device, and partially decentralized control showed a comparable performance. It was confirmed that the control performance could be improved through sharing the sensor’s output data between two control units.

In future research, different input ground motions such as long-period ground motions and near fault ground motions should be considered. An extensive case in which many servers are accommodated on multiple floors in a data center should also be investigated. In addition, a parameter design scheme for other control methods such as sliding-mode control and model predictive control should be studied.

Acknowledgments

This research was supported by a JSPS KAKENHI Grant-in-Aid for Scientific Research (B),

Grant Number 24360230. The authors are deeply grateful to Professor Masaki Takahashi of Keio University for providing constructive comments from the viewpoint of control engineering.

References

- Alhan, C. and Gavin, H.P. (2005), "Reliability of base isolation for the protection of critical equipment from earthquake hazards", *Eng. Struct.*, **27**(9), 1435-1449.
- Anderson, B.D.O. and Moore, J.B. (2005), *Optimal filtering*, Dover Publications, New York, NY, USA.
- Datta, T.K. (2003), "A state-of-the-art review on active control of structures", *ASET J. Earthq. Technol.*, **40**(1), 1-17.
- Fan, Y.C., Loh, C.H., Yang, J.N. and Lin, P.Y. (2009), "Experimental performance evaluation of an equipment isolation using MR dampers", *Earthq. Eng. Struct. Dyn.*, **38**(3), 285-305.
- Fukukita, A. and Takahashi, M. (2011), "Semi-active control for base isolated structure using response evaluator subjected to long-period earthquake ground motion", *J. Syst. Des. Dyn.*, **5**(8), 1674-1686.
- Gavin, H.P. and Zaicenco, A. (2007), "Performance and reliability of semi-active equipment isolation", *J. Sound Vib.*, **306**(1-2), 74-90.
- Hamidi, M. and El Nagggar, M.H. (2007), "On the performance of SCF in seismic isolation of the interior equipment", *Earthq. Eng. Struct. Dyn.*, **36**(11), 1581-1604.
- Kasai, K., Mita, A., Kitamura, H., Matsuda, K., Morgan, T.A., and Taylor, A.W. (2013), "Performance of seismic protection technologies during the 2011 Tohoku-Oki earthquake", *Earthq. Spectra*, **29**(S1), S265-S293.
- Kurata, N., Kobori, T., Takahashi, M., Niwa, N. and Midorikawa, H. (1999), "Actual seismic response controlled building with semi-active damper system", *Earthq. Eng. Struct. Dyn.*, **28**(11), 1219-1467.
- Lambrou, V. and Constantinou, M.C. (1994), "Study of seismic isolation systems for computer floors", Technical Report: NCEER-94-0020, National Center for Earthquake Engineering Research.
- Lin, P.Y., Lin, T.K. and Hwang, J.S. (2013), "A semi-active mass damping system for low- and mid-rise buildings", *Earthq. Struct.*, **4**(1), 63-84.
- Liu, S. and Warn, G.P. (2012), "Seismic performance and sensitivity of floor isolation systems in steel plate shear wall structures", *Eng. Struct.*, **42**(9), 115-126.
- Lu, L.Y. and Lin, G.L. (2008), "Predictive control of smart isolation system for precision equipment subjected to near-fault earthquakes", *Eng. Struct.*, **30**(11), 3045-3064.
- Mei, Z., Peng, Y. and Li, J. (2013), "Experimental and analytical studies on stochastic seismic response control of structures with MR dampers", *Earthq. Struct.*, **5**(4), 395-416.
- Nagashima, I., Maseki, R., Shinozaki, Y., Yoyama, J. and Kohiyama, M. (2011), "Study on performance of semi-active base-isolation system using earthquake observation records", *Proc. International Symposium on Disaster Simulation and Structural Safety in the Next Generation*, Kobe, Japan, Paper No. 8, 7 pages, DVD.
- Naidu, D.S. (2003), *Optimal control systems*, CRC Press, Boca Raton, FL, USA.
- Reggio, A. and De Angelis, Maurizio (2013), "Optimal design of an equipment isolation system with nonlinear hysteretic behaviour", *Earthq. Eng. Struct. Dyn.*, **42**(13), 1907-1930.
- Japan Data Center Council (2013), *Verification and reconsideration of data center facility standard in light of East Japan earthquake disaster*. (in Japanese)
- Shi, Y., Becker, T.C., Furukawa, S., Sato, E. and Nakashima, M. (2013), "LQR control with frequency-dependent scheduled gain for a semi-active floor isolation system", *Earthq. Eng. Struct. Dyn.*, DOI: 10.1002/eqe.2352.
- Simon, D. (2006), *Optimal state estimation: Kalman, H_∞, and nonlinear approaches*, John Wiley & Sons, Hoboken, NJ, USA.
- Spencer, B.F.Jr. (1996), "Recent trends in vibration control in the U.S.A.", *Proceedings of the Third International Conference on Motion and Vibration Control*, Vol. II, Chiba, Japan, K1-K6.

- Spencer, B.F.Jr. and Nagarajaiah, S. (2003), "State of the art of structural control", *J. Struct. Eng.- ASCE*, **129**(7), 845-856.
- Stengel, R.F. (1994), *Optimal control and estimation*, Dover Publications, New York, NY, USA.
- Symans, M.D. and Constantinou, M.C. (1999), "Semi-active control systems for seismic protection of structures: a state-of-the-art review", *Eng. Struct.*, **21**(6), 469-487.
- Villaverde, R. (1997), "Seismic design of secondary structures: state of the art", *J. Struct. Eng. - ASCE*, **123**(8), 1011-1019.
- Xu, Y.L. and Li, B. (2008), "Experimental study of a hybrid platform for high-tech equipment protection against earthquake and microvibration", *Earthq. Eng. Struct. Dyn.*, **37**(5), 747-767.
- Xu, Y.L., Yu, Z.F. and Zhan, S. (2006), "Hybrid platform for high-tech equipment protection against earthquake and microvibration", *Earthq. Eng. Struct. Dyn.*, **35**(8), 943-967.
- Yoshida, K. (2001), "First building with semi-active base isolation", *J. JPN Soc. Mech. Eng.*, **104**(995), 48-52. (in Japanese)
- Yoshida, M., Kohiyama, M. and Takahashi, M. (2012), "Comparative study between centralized and decentralized LQR controls of a building-elevator system", *Proceedings of 15th World Conference on Earthquake Engineering*, Lisbon, Portugal, Paper No. 2819, 10 pages.

IT